Predicted transport properties of liquid plutonium

F. J. Cherne,[1] M. I. Baskes,[1] and B. L. Holian[2]
[1]*MST-8 Structure and Property Relations, Los Alamos National Laboratory, Los Alamos, New Mexico 87545*
[2]*T-12 Theoretical Chemistry and Molecular Physics, Los Alamos National Laboratory, Los Alamos, New Mexico 87545*
(Received 10 January 2003; published 25 March 2003)

The fluid-phase transport properties, diffusivity and viscosity, are calculated by equilibrium and nonequilibrium techniques for plutonium, whose interatomic interactions are described by the modified embedded-atom method. The transport coefficients are evaluated at zero pressure, for temperatures between 950 K and 1300 K. We find the calculated viscosity to be noticeably higher than experiment, while the structure of liquid Pu appears to be similar to other liquid metals.

DOI: 10.1103/PhysRevB.67.092104 PACS number(s): 61.20.Ja, 61.25.Mv, 64.70.Dv, 66.20.+d

The structural behavior of plutonium metal at ambient conditions is arguably the most complex of all elements, since it consists of six allotropic phases between room temperature and its melting point of 913 K. Upon melting, Pu exhibits a volume contraction similar to water and several semi-metals: Bi, Sb, Ge, Si, Ga, and Te.[1] In addition to its unusual properties and its well-known importance to nuclear technologies, Pu can be difficult to work with in the laboratory due to its oxidative, corrosive, reactive, and fissile nature. Thus, the physical properties of the liquid are either unknown (experiments too difficult to perform) or data may be inaccurate (due to impurities or other experimental limitations). Knowledge of the transport properties and the structure of liquid Pu is of great practical interest in casting operations, as well as in its melting and recrystallization behavior.

Recently, the modified embedded-atom method[2] (MEAM) has been applied to describe the interatomic interactions in plutonium.[3] The original embedded-atom method (EAM)[4–7] is based on the local-density approximation, where the electron density in the neighborhood of a nearly free-electron metal ion is assumed to be spherically symmetric. In addition to pairwise-additive forces, an embedding energy, which depends in a nonlinear way on the local electron density, gives a volume dependent, many-body interaction energy. MEAM modifies EAM by including angular dependence and screening in the local electron density. In addition to *s* character, there is *p*-, *d*-, and *f*-characters, as is appropriate to the increased degree of covalent bonding in semimetals, transition metals, and the actinides. The model developed for Pu showed excellent agreement in predicting the energetics of the various allotropic solid phases.[3] Our aim is to apply the MEAM potential to Pu, in order to predict its liquid properties, primarily transport.

Moreover, we suggest that the range of validity of the MEAM interatomic interactions can be extended far beyond the traditional low-temperature, low-pressure solid regime, where semiempirical potentials are fitted to normal density, cohesive energy (preferably as a function of density at zero temperature—the so-called cold curve), elastic constants, and defect energies. Indeed, beyond melting, a more complete description of the interatomic interactions ought to include the mechanical behavior of the fluid, i.e., the linear relationship between stress and strain rate (Navier-Stokes shear viscosity), which is the fluid analog of the linear stress-strain relationship (elastic constants) in solids.

In a recent paper, we showed that MEAM could describe the liquid properties of nickel quite well.[8] Because of the greater inherent complexity of its angular bonding, Pu provides a more interesting test for MEAM. Because of the aforementioned difficulties in working with Pu, there exists a limited amount of experimental data that we can use to validate MEAM Pu in the fluid phase. However, it is encouraging that the melting point predicted by MEAM was found to be within 10% of experiment.[3] Thus, we have every expectation that there exists a parametrization of the MEAM potential for Pu that describes both the solid and liquid phases.

Transport properties in the fluid phase can be computed either from equilibrium fluctuations in molecular-dynamics (MD) simulations, [using Green-Kubo (GK) theory[9,10]], or else from the direct response to external driving in nonequilibrium MD (NEMD). Time-correlation functions of fluxes (velocity for diffusion and shear stress for viscosity) can be evaluated in equilibrium MD simulations of the fluid and integrated in time to get the appropriate transport coefficient. Since the GK method is statistically sensitive to the time origin, we utilize a method of overlapping-time-interval correlation averages,[11] wherein the time interval is chosen such that the initial correlation function has sufficiently decayed to $\approx$20% of its original value. This minimizes the overall length of the simulation, as well as improves the quality of the autocorrelation functions.

Equilibrium calculations for the viscosity and the diffusivity were performed under constant volume and energy conditions, following melting at 2000 K, adjusting the volume to get zero pressure, and equilibrating to the final desired temperature, which usually required $\approx$5 ps. Then 1500 individual correlation functions of lag 2 ps, spaced 0.2 ps apart, were averaged together. We estimated the errors in the calculated diffusivity to be less than 2% and, for the viscosity, less than 12%. (System size was 1024 atoms, and the time step was set to 1 fs.)

We have also applied a new, simple, and much more efficient NEMD method[12] to evaluate the shear viscosity directly, at about 1/10th the computational time required for the GK approach. Traditionally NEMD uses sliding boundary conditions established by Lees and Edwards,[13] as were earlier applied successfully to EAM Ni and Al.[14,15] For our

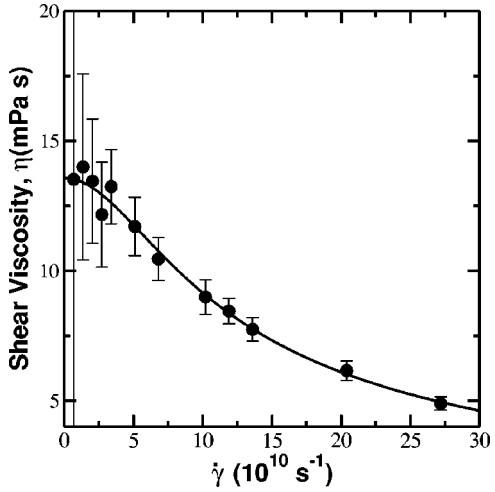

FIG. 1. Lorentzian fit to shear viscosity as a function of shear rate for plutonium at 1200 K.

calculations here, however, using the method outlined by Holian,[12] standard three-dimensional (3D) periodic boundary conditions are imposed, along with a mass-average velocity u_p on one side of the sample, and its opposite on the other side. In order to maintain this flow, an external acceleration $g(t)$ is applied to each atom (in the direction of the velocity u_p), which can be obtained from the forces summed up on each side of the sample. The result is a sinusoidal velocity profile predicted from Navier-Stokes hydrodynamics. The kinematic viscosity, $\nu=\eta/\rho$ (η is the shear viscosity and ρ is the density of the fluid), can then be obtained

$$\nu=-\frac{\overline{g^{ss}}w^2}{\pi^2 u_p}, \tag{1}$$

where $\overline{g^{ss}}$ is the steady-state time-averaged driving acceleration, and w is half the width of the periodic box. The shear viscosity at several shear rates ($\dot{\gamma}=2u_p/w$) is extrapolated to obtain the GK limit at zero shear rate, using the generalized Lorentzian functional form[12,16]

$$\eta=\frac{\eta_0}{[1+(\tau\dot{\gamma})^2]^{\mu/2}}, \tag{2}$$

where η_0 is the shear viscosity at zero shear rate, τ is the shear-thinning relaxation time, and μ is a constant. (Results were fitted by weighted nonlinear least squares, where the weights are $1/\sigma^2$; σ is the standard deviation of η at a given $\dot{\gamma}$.) An example of this fitting process is given in Fig. 1. Note that the error increases significantly with decreasing shear rate. The fits yielded values of μ from 0.72 to 0.84 over the temperature range of 950 K to 1300 K. The shear-thinning relaxation time, τ decreased uniformly from 19 ps to 10 ps from 950 K to 1300 K.

The system size for our NEMD simulations was 2048 atoms in a box of approximate dimensions $54\times40\times24$ Å, which gives a density appropriate to zero pressure at zero shear rate (as long as the length in the x direction was greater than about 35 Å, results were reliable). Temperature was

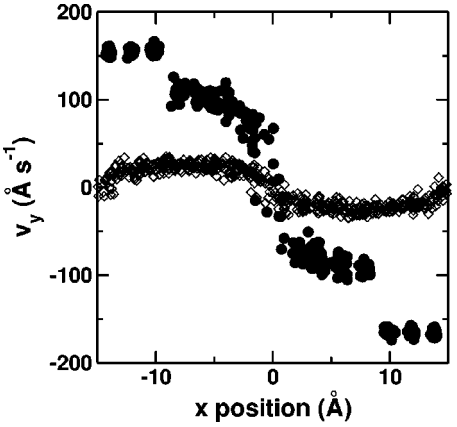

FIG. 2. Velocity profile in the y direction as a function of the x-position for MEAM Ni. Open symbols represent a low shear rate (1.3×10^{12} s^{-1}), where the velocity profile is sinusoidal; solid symbols are for a high shear rate (6.6×10^{12} s^{-1}), where a solid-like columnar (or liquid-crystal-like) structure develops.

maintained with a Nosé-Hoover thermostat,[17] and the timestep was set to 1 fs. The simulations were allowed to equilibrate at the desired shear rate for 5 ps before averaging the driving force over 15 ps. We estimate the errors in the viscosity to be less than 7%.

As can be seen in Fig. 2, at low shear rates, the flow is the expected Navier-Stokes sinusoidal velocity profile. At the lowest rates, standard deviations are large(See Fig. 1). However, at very high shear rates, the system develops a solid-like columnar structure, as shown for Ni in Fig. 2. Since this is far from the Navier-Stokes regime, we can hardly expect to include it in the extrapolation to the GK limit. We applied this method to MEAM Ni (Ni4 in Ref. 8) and found the extrapolated NEMD value for the zero shear rate viscosity to coincide with GK results to within 3%. Adjusting the strain rates using the mass ratio between Pu and Ni, we chose to extrapolate the Pu data using shear rates from 3.7×10^9 s^{-1} to 2.2×10^{11} s^{-1}. In Table I we present the heat of solidification ΔH, relative volume change on melting $\Delta V/V$, melting point T_m, liquid density ρ, temperature derivative of the liquid density $\partial\rho/\partial T$, and liquid specific heat C_p for MEAM Pu.[3] Most of these agree well with experiment, apart from $\Delta V/V$. Although $\Delta V/V$ is about twice experiment, MEAM ε-Pu shows expansion upon solidifying, as does experiment.

In Table I we show a recalculation of the zero-pressure melting temperature (T_m) compared to experiment, using the

TABLE I. Thermo-physical properties of the liquid and solid-liquid transformation predicted by the parameters given in Ref. 3.

Thermo-physical properties	Calculated	Experimental
ΔH (eV/atom)	0.025	0.029
$\Delta V/V$ (%)	−5.9	−2.5
T_m (K)	918±5	913
ρ (g/cm^3) at 913 K	17.29	16.62
$\partial\rho/\partial T$ (mg/cm^3 K)	−2.0	−1.5
C_p (J/K mol) at 1000 K	46.8	41.8

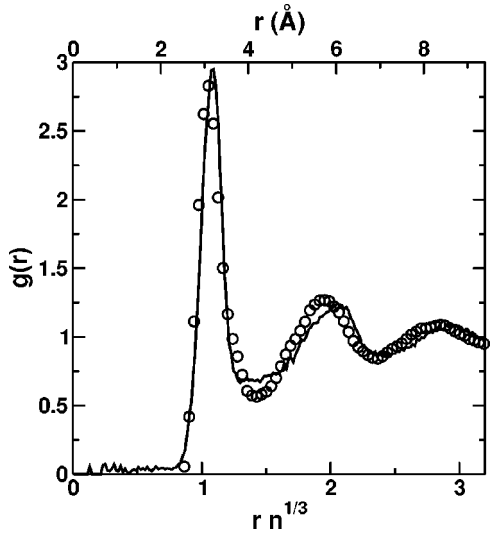

FIG. 3. Radial distribution function g(r) of MEAM Pu (solid line) at 950 K for distance r scaled by the cube root of the number density n, compared with the experimental RDF for Al (symbols) at 943 K. The upper axis gives r for Pu.

moving interface method.[3] Rather than determining T_m by extrapolating the velocity of the solid-liquid interface to zero, we constructed a two-phase cell from a series of constant volume and energy simulations. The result is remarkably close to the experimental melting point.

In Fig. 3, we present the radial distribution function (RDF) for liquid Pu at 950 K, calculated by taking the average of 10 configurations spaced 0.1 ps apart. Typically in the RDF of a liquid, the distance to the first peak is approximately the nearest-neighbor distance in the phase prior to melting: for ε-Pu, the bcc phase prior to melting, the first peak is at 3.14 Å. Indeed, we see that the first peak in MEAM liquid Pu occurs at 3.175 Å. (If α-Pu were present we would expect to see a peak at 2.58 Å.) Note that since there is no peak at short ($\sim$2.6 Å) atomic separation, the number of Pu dimers in the liquid must be very low. We also present in Fig. 3 the experimental RDF for aluminum, which has a similar melting point to Pu. Obviously, there is nothing strikingly ''peculiar'' about the structure of liquid MEAM Pu.

In Fig. 4, we show the calculated self-diffusivity in liquid MEAM Pu, which obeys the Arrhenius form

$$D(T) = D(T_m)\exp\left[-\frac{E_D}{k}\left(\frac{1}{T}-\frac{1}{T_m}\right)\right]. \tag{3}$$

where D is the diffusion coefficient, E_D is a diffusional activation energy, k is Boltzmann's constant, and T is the temperature (the melting temperature is T_m). The resulting values for liquid MEAM Pu are given in Table II.

Experimental data for liquid Pu viscosity[18] is compared to MEAM Pu in Fig. 4. NEMD results are extrapolated to zero shear rate, in excellent agreement with equilibrium GK results. Viscosity as a function of temperature can also be fitted to an Arrhenius expression

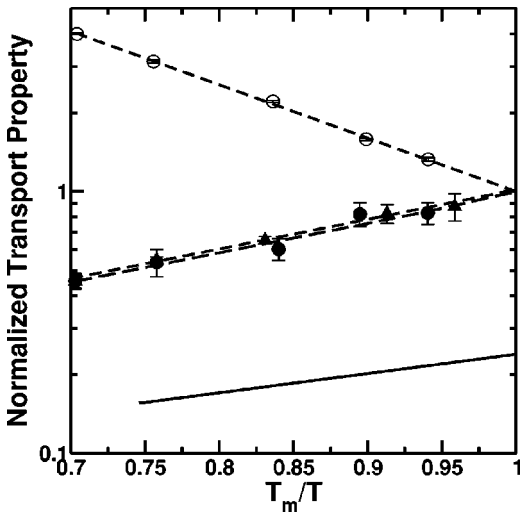

FIG. 4. Diffusivity and viscosity of liquid MEAM Pu as a function of temperature. The diffusivity and viscosity are normalized to the GK value at the melting temperature. The diffusivity is depicted by the open circles. Viscosity (at zero shear rate) as calculated by NEMD (triangles) and GK (circles) methods are depicted by the solid symbols. The dashed lines represent an Arrhenius fit through the calculated data. The experimental viscosity is represented by the solid line.

$$\eta(T) = \eta(T_m)\exp\left[\frac{E_\eta}{k}\left(\frac{1}{T}-\frac{1}{T_m}\right)\right], \tag{4}$$

where values for the parameters $\eta(T_m)$ and E_η are tabulated in Table II. The fit was weighted using the errors associated with the data, which for the NEMD simulations is less than 2%, and less than 7% for the equilibrium GK results. Note that the GK method would require an order of magnitude more computing time, in order to reduce its errors to that of NEMD.

Before turning to the comparison of experiment and theory, we make the following interesting observation about MEAM Pu. Since the diffusivity is so well-represented by Eq. (3) and viscosity by Eq. (4), we see that the model liquid obeys the classic Stokes-Einstein relationship over the limited temperature range studied, i.e.,

$$\frac{D(T)\,\eta(T)}{kT\sqrt[3]{n(T)}} = \frac{D(T_m)\,\eta(T_m)}{kT_m\sqrt[3]{n(T_m)}} \approx \text{const.} \tag{5}$$

TABLE II. Arrhenius fits to the diffusivity and viscosity data presented in Fig. 4 where E is the activation energy in eV/atom, $\eta(T_m)$ is the viscosity at melting in mPa-s and $D(T_m)$ is the diffusivity at melting in cm^2/s.

Method	E_η	$\eta(T_m)$	E_D	$D(T_m)$
NEMD	0.205	25.2		
EMD	0.208	24.8	0.37	2.3 x 10^{-6}
expt.[a]	0.133	5.93		

[a]Reference 18.

where n is the number density. We determine that the const. in Eq. (5) is 0.154 ± 0.0123 or $\approx 1/2\pi$. This value is significantly greater than the $1/6\pi$ predicted by the Stokes-Einstein expression or the $1/4\pi$ predicted by the Sutherland-Einstein expression.

The temperature variation of the calculation and experiment are similar, but the calculated values are a factor of four larger than experiment. The experimental methods employed are known to produce errors by as much as 30%;[19] hence, it is extremely unlikely that experimental errors are sufficient to explain the disparity between the calculated and experimental results. It is also unlikely that surface oxides or impurities could affect the experimentally measured Pu viscosity by a factor of four. The most likely source of discrepancy is the MEAM potential for Pu, which had no input from liquid-phase data for its parameters. In an earlier paper,[8] the authors observed significant variation in viscosity between a number of potentials produced for Ni. Preliminary calculations have shown that when the angular screening value is reduced to 0.8 the calculated viscosity was lowered by as much as an order of magnitude. However, the melting point was reduced significantly. This strong dependence of liquid transport properties on potential presents a unique opportunity to use information about the mechanical response of the fluid to improve the range of validity of the MEAM treatment of interatomic interactions.

We thank Steve Valone (Los Alamos) and Ramon Ravelo (University of Texas, El Paso) for useful discussions. Work at Los Alamos was invariably supported by the U.S. Department of Energy under Contract No. W-7405-ENG-36.

[1] M. Boivineau, J. Nucl. Mater. **297**, 97 (2001).
[2] M.I. Baskes, Phys. Rev. B **46**, 2727 (1992).
[3] M.I. Baskes, Phys. Rev. B **62**, 15 532 (2000).
[4] M.S. Daw and M.I. Baskes, Phys. Rev. Lett. **50**, 1285 (1983).
[5] M.S. Daw and M.I. Baskes, Phys. Rev. B **29**, 6443 (1984).
[6] M.S. Daw, S.M. Foiles, and M.I. Baskes, Mater. Sci. Rep. **9**, 251 (1993).
[7] S.M. Foiles, M.I. Baskes, and M.S. Daw, Phys. Rev. B **33**, 7983 (1986).
[8] F.J. Cherne, M.I. Baskes, and P.A. Deymier, Phys. Rev. B **65**, 024209 (2002).
[9] M.S. Green, J. Chem. Phys. **20**, 1281 (1952).
[10] M.S. Green, J. Chem. Phys. **22**, 398 (1954).
[11] D.C. Rapaport, *The Art of Molecular Dynamics Simulation* (Cambridge University Press, Cambridge, UK, 1995).
[12] B.L. Holian, J. Chem. Phys. **117**, 1173 (2002).
[13] A.W. Lees and S.F. Edwards, J. Phys. C **5**, 1921 (1972).
[14] F.J. Cherne and P.A. Deymier, Scr. Mater. **39**, 1613 (1998).
[15] F.J. Cherne and P.A. Deymier, Scr. Mater. **45**, 985 (2001).
[16] S. Bair, C. McCabe, and P.T. Cummings, Phys. Rev. Lett. **88**, 058302 (2002).
[17] S. Nosé, Prog. Theor. Phys. Suppl. **103**, 1 (1991).
[18] L.J. Wittenberg, D. Ofte, and W.G. Rohr, Nucl. Appl. Technol. **3**, 550 (1967).
[19] T. Iida and R.I.L. Guthrie, *The Physical Properties of Liquid Metals* (Clarendon Press, Oxford, 1988).